# System identification applied to stiction quantification in industrial control loops: A comparative study☆

Riccardo Bacci di Capaci[a,b], Claudio Scali[a], Gabriele Pannocchia[a]

[a]*Department of Civil and Industrial Engineering, University of Pisa, Italy*
[b]*Corresponding author, e-mail: riccardo.baccidicapaci@for.unipi.it*

**Abstract**

A comparative study of different models and identification techniques applied to the quantification of valve stiction in industrial control loops is presented in this paper, with the objective of taking into account for the presence of external disturbances. A Hammerstein system is used to model the controlled process (linear block) and the sticky valve (nonlinear block): five different candidates for the linear block and two different candidates for the nonlinear block are evaluated and compared. Two of the five linear models include a nonstationary disturbance term that is estimated along with the input-to-output model, and these extended models are meant to cope with situations in which significant nonzero mean disturbances affect the collected data. The comparison of the different models and identification methods is carried out thoroughly in three steps: simulation, application to pilot plant data and application to industrial loops. In the first two cases (simulation and pilot plant) the specific source of fault (stiction with/without external disturbances) is known and hence a validation of each candidate can be carried out more easily. Nonetheless, each fault case considered in the previous two steps has been found in the application to a large number of datasets collected from industrial loops, and hence the merits and limitations of each candidate have been confirmed. As a result of this study, extended models are proved to be effective when large, time varying disturbances affect the system, whereas conventional (stationary) noise models are more effective elsewhere.

*Keywords:* Control loop performance monitoring, stiction quantification, Hammerstein system identification, disturbance estimation

## 1. Introduction

Oscillations in control loops cause many issues which can disrupt the normal plant operation. Typically fluctuations increase variability in product quality, accelerate equipment wear, move operating conditions away from optimality, and generally they cause excessive or unnecessary energy and raw materials consumption. The common sources for oscillatory control loops can be found in poor design of the process and of the control system, e.g. choice and pairing of controlled and manipulated variables, from one hand. From another hand, poor controller tuning, oscillatory external disturbances, and control valve nonlinearities such as stiction, backlash and saturation, are frequent causes of excessive loop oscillations. Therefore, control loop monitoring and assessment methods are recognized as important means to improve profitability of industrial plants. An effective monitoring system should, first of all, detect loops with poor performance. Then, for each faulty loop, it should indicate the sources of malfunction (among possible causes) and suggest the most appropriate way of correction.

Among actuator problems, valve stiction is said to be the most common cause of performance degradation in industrial loops [2]. An extensive characterization of this phenomenon was firstly given in [3]. Two kinds of models are commonly used to describe stiction: models derived from physical principles and models derived from process data. Physical models are more accurate, but owing to the large number of unknown parameters, they may not be convenient for practical purposes [4, 5]. This is the main reason why data-driven models are typically preferred [3, 6, 7, 8, 9].

A review of a significant number of stiction detection techniques recently presented in the literature is reported in [2]; among them: cross-correlation function-based [10], waveform shape-based [7, 11, 12, 13, 14, 8, 15], nonlinearity detection-based [16], and model-based algorithms [17]. In [2] a comparison of performance is also presented by applications on a large benchmark (93 loops) of industrial data.

Following their conclusions, research on stiction *modeling* and *detection* (i.e. confirmation of its presence) has to be considered a mature topic, even if it may happen that different results are obtained once applied on the same industrial dataset, owing to complexity and superposition of different phenomena. Stiction *quantification* instead has to be regarded as an area where research contributions are still needed. The main difficulty in quantifying the amount of stiction arises from the fact that the valve stem position (MV) is not measured and recorded in many (old designed) industrial control systems [18], and then it must be reconstructed from available measurements (controlled variable, PV, and controller output, OP) by using a data driven stiction model.

☆A preliminary version of this paper has been presented in [1].

In stiction quantification techniques, the control loop is often modeled by a Hammerstein system: a nonlinear block for valve stiction, followed by a linear block for the process. This approach was firstly used in [19] along with a one parameter stiction model given in [6]. However this method may not capture the true stiction behavior since the nonlinear model is not always very accurate. Subsequently, other techniques have been proposed [20, 21, 22, 23]. A specific linear model was used in [17], which also accounts for nonstationary disturbances entering the process. The control loop was modeled as a Hammerstein-Wiener structure also in [24]. More recently, a technique based on harmonic balance method and describing function identification was proposed in [25]. A simplified method based on a new semi-physical valve stiction model was illustrated in [26].

A recent paper by the authors [18] pointed out that, while simulation is the first necessary step to check mathematical consistency of a proposed identification technique, its validation on a single set of industrial data can be pointless due to the superposition of unknown effects, such as nonstationary disturbances. As a confirmation, results obtained by different quantification techniques can be very inconsistent once applied on the same set of industrial data (as it happened in benchmark presented by [2], Chp. 13). To overcome this problem, it is suggested in [18] to repeat stiction estimation for different data acquisitions for the same valve, in order to follow the time evolution of the phenomenon and to disregard anomalous cases (outliers). The comparison of reasonable values of stiction with predefined acceptable thresholds allows one to schedule valve maintenance in a reliable way (on-line stiction compensation is also an alternative, though not very popular in industry).

Following the above considerations, this paper represents a continuation of the work reported in [18], and addresses the following new objectives: i) to compare some different identification techniques (of the linear model in the Hammerstein system) when applied on the same dataset; ii) to show how external nonstationary disturbances can influence stiction estimation and system identification. Both aspects were not considered in the methodology presented in [18] where a single (ARX) model structure and a single identification technique were considered, and nonstationary disturbances were not modeled. Preliminary results of this study were reported in [1][1].

The remainder of this paper is organized as follows. In Section 2, five different models and identification methods of the linear block (in the Hammerstein system) and two models for the stiction nonlinearity are illustrated. The merits of each model and identification method are firstly assessed in simulation in Section 3, and then validated in a pilot plant in Section 4. Section 5 is dedicated to applying and evaluating the different techniques to several industrial data sets. Finally, conclusions are drawn in Section 6.

[1]The present paper extends these previous results in an application-oriented direction. Different simulation examples and new datasets of pilot plant are now illustrated, and, mostly, results obtained from several registrations of industrial control loops are shown.

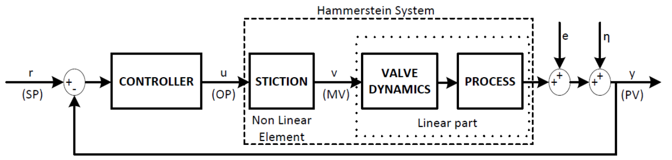


Figure 1: Hammerstein system representing the (sticky) control valve followed by the linear process, inserted into the closed-loop system.

## 2. Hammerstein system: models and identification method

In this work, the control loop is modeled by a Hammerstein system as depicted in Figure 1. Two well-established stiction models are used to describe the nonlinear valve dynamics: Kano's [7] and He's [8] model. Five different models describe the linear process dynamics: ARX (Auto Regressive model with eXternal input), ARMAX (Auto Regressive Moving Average with eXternal input), SS (State Space model), EARX (Extended Auto Regressive model with eXternal input), EARMAX (Extended Auto Regressive Moving Average with eXternal input, [27]).

### 2.1. Nonlinear stiction models

In Kano's stiction model [7], the relation between the controller output (the desired valve position) OP and the actual valve position MV is described in three phases (Figure 2):

I. *Sticking*: MV is steady (*A*-*B*) and the valve does not move, due to static friction force (dead-band + stick-band, *S*).

II. *Jump*: MV changes abruptly (*B*-*C*) because the active force unblocks the valve, which jumps of an amount *J*.

III. *Motion*: MV changes gradually, and only the dynamic friction force can possibly oppose the active force; the valve stops again (*D*-*E*) when the force generated by the control action decreases under the stiction force.

In He's stiction model the relation between OP and MV is slightly different and simpler [8]. The model uses static $f_S$ and dynamic $f_D$ friction parameters and is closer to the first-principle-based formulation. It uses a temporary variable that represents the accumulated static force. Note that parameters of He's model have their equivalent in Kano's model and vice versa, according to the following equations (cf. also Figure 2):

$$\begin{cases} S = f_s + f_d \\ J = f_s - f_d \end{cases} \quad \text{or} \quad \begin{cases} f_s = \dfrac{S+J}{2} \\ f_d = \dfrac{S-J}{2} \end{cases} \tag{1}$$

However, due to different logics, the two stiction models can generate different MV sequences for a given OP and with equivalent parameters. Note also that Kano's and He's models are quite simple, since they imply uniform stiction parameters for the whole valve span. Stiction could be really inhomogeneous, having various amounts for different operating conditions (that

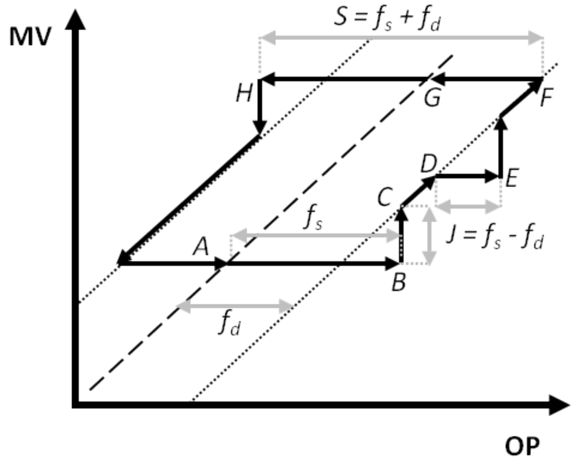


Figure 2: Valve stiction: theoretical behavior of MV vs. OP, and graphical representation of Kano's and He's model parameters.

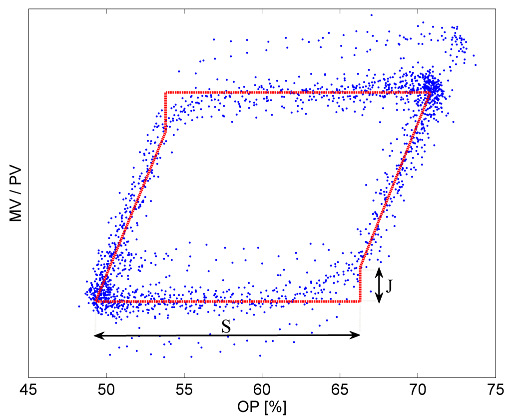


Figure 3: Valve stiction: typical industrial behavior of PV vs. OP.

is, different OP values) and then producing complicated signatures on MV(OP) diagram. In order to overcome these limitations, recent works which implement flexible stiction models have been proposed [28, 29].

Valve stiction produces an offset between controlled variable PV and Set Point SP, and this causes loop oscillations because the valve is stuck even though the integral action of the controller increases (or decreases) OP. The MV(OP) diagram shows a parallelogram-shaped limit cycle, while MV(OP) would be perfectly linear without valve stiction. Figure 3 represents the PV(OP) plot for a case of flow rate control loop, for which the fast linear dynamics allows one to approximate MV(OP) with PV(OP), since MV is usually not measured. Figure 3 shows also the signature obtained with Kano's stiction model by fitting the industrial data.

It should be recalled that also in the case of stiction, loops with slower dynamics (level control, temperature control) usually show PV(OP) diagrams having elliptic shapes. Similar PV(OP) diagrams are obtained for other types of oscillating loops (external stationary disturbance or aggressive controller tuning), and therefore assigning causes is not straightforward.

It is also worth saying that the value of $J$ is critical to induce limit cycles [20, 21]. In addition, while $S$ can be often easily recognized on PV(OP) diagram, since limit cycles show clear horizontal paths, on the opposite, the process dynamics or the presence of high level noise make PV trend deviate significantly from MV trend, and make $J$ almost hidden [2] (see Figure 3).

Finally, note that $S \simeq 1\%$ is considered enough amount of stiction to cause performance problems [2]. Increasing the amount of stiction (associated to the ratio $S/J$), the amplitude and the period of oscillation of OP and PV signals increase significantly, thus leading to particularly poor performance. For these reasons, being able to quantify and predict the evolution of stiction in time is important in order to schedule maintenance action on more critical valves.

### 2.2. *Linear process models*

The linear part of the Hammerstein system has one of the following structures, in discrete-time form.

- ARX:

$$A(q)y_k = B(q)v_{k-t_d} + e_k \tag{2}$$

  where $v_k$ and $y_k$ are the linear process input and output (that is, MV and PV respectively); $A(q)$ and $B(q)$ are polynomials in time shift operator $q$ (i.e. such that $q\,v_k = v_{k+1}$), and given as:

$$\begin{aligned} A(q) &= 1 + a_1 q^{-1} + a_2 q^{-2} + \ldots + a_n q^{-n} \\ B(q) &= b_1 q^{-1} + b_2 q^{-2} + \ldots + b_m q^{-m} \end{aligned} \tag{3}$$

  where $e_k$ is white noise, $t_d$ is the time delay of the process, $(n,m)$ are the orders on the auto-regressive and exogenous terms, respectively.

- ARMAX:

$$A(q)y_k = B(q)v_{k-t_d} + C(q)e_k \tag{4}$$

  where $A(q)$ and $B(q)$ are defined in (3), whereas:

$$C(q) = 1 + c_1 q^{-1} + c_2 q^{-2} + \ldots + c_p q^{-p} \tag{5}$$

  in which $p$ is the order of the moving average term.

- SS:

$$\begin{aligned} x_{k+1} &= \mathbf{A}x_k + \mathbf{B}v_k + \mathbf{K}e_k \\ y_k &= \mathbf{C}x_k + e_k \end{aligned} \tag{6}$$

  where $\mathbf{A} \in \mathbb{R}^{n\times n}$, $\mathbf{B} \in \mathbb{R}^{n\times 1}$, $\mathbf{C} \in \mathbb{R}^{1\times n}$, $\mathbf{K} \in \mathbb{R}^{n\times 1}$, and $n$ is the model order.

- EARX:

$$A(q)y_k = B(q)v_{k-t_d} + e_k + \eta_k \tag{7}$$

  where $\eta_k$ is a time varying bias representing the additive nonstationary external disturbance, to be estimated along with the polynomials $A(q)$ and $B(q)$ (see Figure 1).

- EARMAX:

$$A(q)y_k = B(q)v_{k-t_d} + C(q)e_k + \eta_k \tag{8}$$

## 2.3. Hammerstein system identification

The proposed stiction quantification techniques are based on a grid search over the space of the nonlinear model parameters. The computational time of the methodology may be long, but it does not represent a disadvantage for three main reasons: the procedure is oriented toward an off-line application which requires data registered for hours, the wear phenomena in valves occur slowly (weeks or months), and valve maintenance usually occurs periodically on the occasion of a plant shutdown.

In details, the system identification is carried out according to the following procedure. (i) A 2-D grid of stiction parameters $(S,J)$ is built; for each possible combination of $(S,J)$, MV signal is generated from (measured) OP using Kano's model. For He's model, MV is generated using the corresponding parameters $(f_s, f_d)$ according to (1). (ii) Coefficients of the linear models are identified using different techniques on the basis of (generated) MV and (measured) PV sequences.

The overall model fit is quantified by $F_{PV}$:

$$F_{PV} = 100 \cdot \left(1 - \frac{\|PV_{est} - PV\|^2}{\|PV - PV_m\|^2}\right) \tag{9}$$

where $PV$, $PV_m$ and $PV_{est}$ are vectors containing values of the measured output, measured output average and estimated output sequences, respectively. The symbol $\|\cdot\|$ denotes the Euclidean norm. Thus, for each considered linear model, the optimal combination of $(S,J)$ is computed as the one that maximizes the fitting index $F_{PV}$.

Note that the stiction parameters grid has a triangular shape, since $f_s \geq f_d \geq 0$ (or $S \geq J$). Thus, overshoot stiction cases $(J > S)$ are excluded; actually waveforms generated for these combinations are rarely observed in practice. The largest value of $S$ (and $J$) is the OP oscillation span. Therefore, under boundary conditions, when $S = J = \Delta OP$ (the span of OP), the valve jumps between two extreme positions, generating an exactly squared MV signal. Note that computational time is roughly halved by the use of a triangular-shaped grid.

ARX model coefficients are identified by least-squares regression. SS model coefficients are estimated using a subspace identification method, the PARSIM-K technique [30]. ARMAX, EARX and EARMAX models are identified using the recursive least-squares (RLS) identification algorithm proposed (for EARMAX model) by [27]. For EARX and EARMAX, a decoupled parameter covariance update procedure with variable forgetting factors is developed to identify the process parameters and the bias term [27]. To the best of the authors' knowledge, this is the first time that a SS model and an EARX model are used for Hammerstein system identification applied to valve stiction estimation.

## 2.4. Specific issues in identification of the Hammerstein stiction and process system

It is worth to underline that the exact stiction estimates depend on several issues. In addition to some general aspects (e.g., the dataset used in identification, choice of loss function, identification algorithm), in the case of Hammerstein system identification with grid search algorithm, also the following issues are important: type, order, and time delay of the linear (process) model; type of the nonlinear (stiction) model; step size of the grid. Only some of these aspects will be analyzed hereinafter in the text.

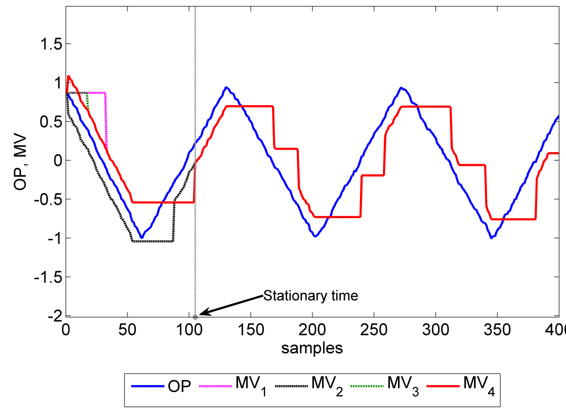


Figure 4: Ambiguity in the nonlinear model initialization (data of CHEM 10, benchmark of [2]).

Moreover, the way in which the stiction model is initialized must be attended. This issue could seem a negligible aspect, but in reality, as it has been verified by a large number of simulations and applications, it is an important point, as discussed next and in the application results. In particular, the identification results can be sensitive to the initialization of the Kano's model. On the opposite, the He's model does not present these problematics.

Given an OP sequence and fixed $(S,J)$ parameters, different MV sequences can be produced, simply by changing the initial values of the auxiliary parameters of the Kano's model: $u_s, stp, d$ [7]. Figure 4 shows that, for the same triangular OP wave, given a combination of stiction parameters $(S = 1, J = 0.5)$, four different MV sequences can be generated using different values of *stp* and $d$. Only after several samples, all MV sequences coincide perfectly with each other.

This *stationary time* depends on the specific OP sequence and the $(S,J)$ combination. Therefore, during the identification procedure, three choices are possible for the initialization of Kano's model states:

In.1 The auxiliary variables are initialized arbitrarily, the same for each combination;

In.2 A threshold stationary time is fixed *a priori* and an average MV sequence is considered after this time;

In.3 The stationary time is computed for each $(S,J)$ combination and only the steady sequence of MV is considered.

According to the results of extensive simulations that have been carried out, the third (or at least the second) choice should be preferred.

## 3. Simulation study

The objective of this section is to investigate the impact of different factors on the effectiveness of the methods to yield accurate estimation. To this aim, simulation results are provided to describe the capabilities of the compared algorithms for Hammerstein system identification. The systems are simulated in closed-loop operation, which is known to be a difficult task as compared to open-loop identification, because of the correlation between process noise and input sequences. OP and PV sequences are used without any filtering in the identification methodologies, which fall under the class of direct identification techniques.

### 3.1. Effect of stiction and disturbance amount

Firstly, the impact of stiction and external disturbance amount is investigated. The following ARMAX process, with $(n,m,p) = (3,3,3)$ and subject to an external disturbance, is considered in discrete-time form:

$$\begin{aligned} y_k = {} & 0.5215 y_{k-1} - 0.0590 y_{k-2} + 0.0009 y_{k-3} \\ & + 0.2836 u_{k-1} + 0.2442 u_{k-2} + 0.0088 u_{k-3} \\ & + e_k + 0.5 e_{k-1} + 1.0 e_{k-2} - 1.0 e_{k-3} + \eta_k \end{aligned} \tag{10}$$

where $\eta_k$ is the external (unmeasured) disturbance given by:

$$\eta_k = a\big(sin(0.03\,k) + 0.5 sin(0.07\,k)\big) \tag{11}$$

with $a \geq 0$. Stiction parameters are varied to cover a wide range of phenomena ($S \in [1, 12]$, $J \in [0.5, 4]$) using Kano's model. The stationary disturbance $\{e_k\}$ is a normally distributed white noise signal with standard deviation $\sigma_e$ = 0.1. The process is in closed-loop with a Proportional-Integral (PI) controller having the following transfer function $C_{PI}(q) = K_c + \frac{K_I}{1-q^{-1}}$, with proportional gain $K_C = 0.5$ and integral gain $K_I = 0.5$ (values which allow stable response with acceptable performance).

The system is excited by introducing a random-walk signal, as controller set-point, which varies as follows:

$$SP_k = \begin{cases} SP_{k-1} + \Delta(R_{2k} - 0.5) & \text{if} \quad R_{1k} > 1 - \delta_{sw} \\ SP_{k-1} & \text{otherwise} \end{cases} \tag{12}$$

where $\Delta$ is a positive scalar, $\delta_{sw}$ is the average switching probability and $R_{1k}$, $R_{2k}$ are two random numbers drawn, at time $k$, from a uniform distribution in $[0,1]$. For simulation purposes, the following parameters have been set: $\Delta = 2$ and $\delta_{sw} = 0.05$. This type of set-point is thought to reproduce an industrial scenario of a control loop with variable reference commanded by a higher-level Model Predictive Controller.

One hundred Monte-Carlo simulations are carried out, using different realizations of white noise $\{e_k\}$, for each set of stiction parameters and disturbance amplitude. The orders and the time delay of the linear process models are fixed a-priori in performing identification steps, namely $t_d = 0$, $(n,m) = (2,2)$ for ARX and EARX, $(n,m,p) = (2,2,2)$ for ARMAX and EARMAX, $n = 2$ for SS. Therefore a little mismatch in the orders of the linear part is present. Conversely no structural error is present in the nonlinear part: Kano's model is also used to generate MV sequences.

The first two-thirds of data are used as identification data set; the last third of data is used as validation set in order to test the models previously identified. As in (9), a fitting index for the estimation data set, $F_{PV}^{(id)}$, and for the validation data set, $F_{PV}^{(val)}$, can be defined.

The linear model fit is quantified by the scalar $E_G$ given as:

$$E_G = 100 \cdot \left(1 - \frac{\|G_{est}(z) - G(z)\|_\infty}{\|G(z)\|_\infty}\right) \tag{13}$$

where $G(z)$ and $G_{est}(z)$ are the true process and the identified model discrete-time transfer functions, respectively, and $\|g(z)\|_\infty = \max_{\omega\in[0,2\pi]} |g(e^{i\omega})|$.

The nonlinear model fit is quantified by $F_{MV}$:

$$F_{MV} = 100 \cdot \left(1 - \frac{\|MV_{est} - MV\|^2}{\|MV - MV_m\|^2}\right) \tag{14}$$

where $MV$, $MV_m$ and $MV_{est}$ are vectors containing values of the actual valve position, average actual valve position and the estimated valve position.

Figure 5 shows a summary of the results for the case of $a = 0$ in (11), that is, when valve stiction is the only source of loop oscillation. Top panels show the various simulated stiction cases $(S,J)$ and the corresponding estimated parameters $(S_{id}, J_{id})$. Bottom panels show the values of the fitting indices $E_G$ and $F_{PV}^{(val)}$ using the different proposed techniques. Figure 6 shows a summary of the results for the case of $a = 0.25$ in (11), that is, when an external disturbance acts simultaneously with valve stiction.

It can be clearly seen that, in the case of pure stiction oscillation ARX, ARMAX and SS models ensure a more accurate stiction estimation and, mostly, perform a better linear model identification: $E_G$ values are higher. On the other hand, in the presence of external disturbance, the stiction parameters and the linear model identified using EARMAX and EARX are of higher accuracy as compared to the other identification techniques: $E_G$ and $F_{PV}^{(val)}$ values are higher. Moreover, the little mismatch in the orders of the linear model does not sensibly affect the results.

Note that, both in the case of only stiction and in the case of additive disturbance, a worse model identification arise because $J$ is not perfectly estimated, whereas $S$ is always well estimated. Higher values of $F_{PV}^{(val)}$ are obtained for higher values of $S$. When the amount of stiction increases (that is, the ratio $S/J$), the amplitude of oscillation increases. Therefore, since the stationary disturbance $\{e_k\}$ has the same standard deviation for each simulation, the higher is stiction, the lower is the noise-to-signal ratio. Anyway, noise-to-signal ratio is significant for all the considered simulations, by ranging in the following interval: $NSR \in [5, 25\%]$.

The effect of magnitude of the external disturbance ($\eta$) is further evaluated. The same linear process of (10) is studied, and valve stiction is described by Kano's model with $S = 5$ and $J = 2$. The external disturbance is as in (11) with $a \in [0, 1]$.

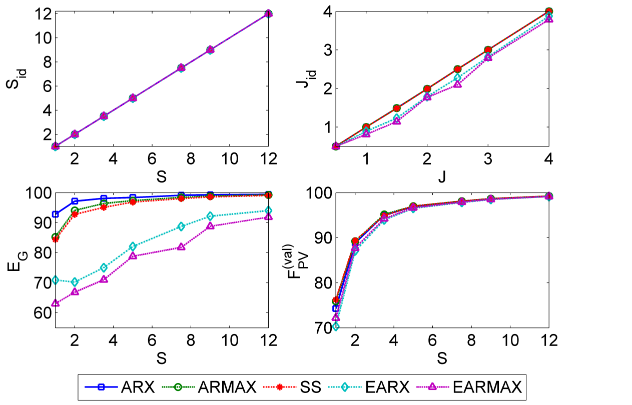


Figure 5: Simulation example: identification results in absence of the external disturbance ($a = 0$). Top panel, left: $S_{id}$ vs $S$, right: $J_{id}$ vs $J$; bottom panel, left $E_G$ vs. $S$, right $F_{PV}^{(val)}$ vs. $S$.

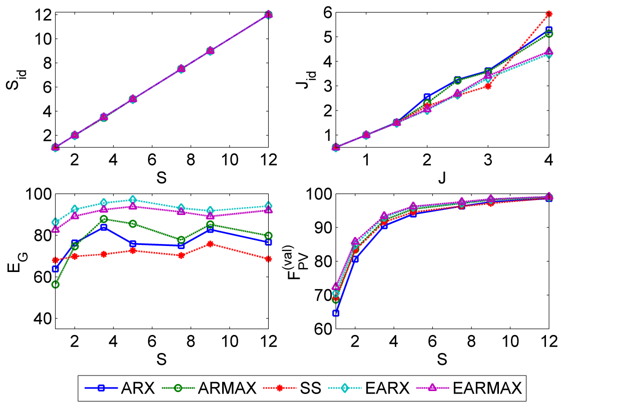


Figure 6: Simulation example: identification results in the presence of external disturbance ($a = 0.25$). Top panel, left: $S_{id}$ vs $S$, right: $J_{id}$ vs $J$; bottom panel, left $E_G$ vs. $S$, right $F_{PV}^{(val)}$ vs. $S$.

Overall, 10 different values of magnitude of disturbance are considered, that is, 10 different combinations of the two sinusoidal waves that form $\eta$. For each level of $a$, and for the five different types of linear process model, one hundred Monte-Carlo (MC) simulations are carried out, by using different realizations of white noise $\{e_k\}$. The PI controller has the following fixed parameters: $K_c = 0.5$ and $K_i = 0.5$. The same procedure of identification adopted for Figures 5 and 6 is employed.

Figure 7 shows a summary of the results for different levels of disturbance. Top panels show the estimates of stiction parameters $(S_{id}, J_{id})$, while bottom panels show values of the fitting indices ($E_G$ and $F_{PV}^{(val)}$) for different values of $a$. It can be clearly seen that the higher is the amplitude of disturbance, the lower is the identification accuracy of the linear model ($E_G$) and the global fitting index ($F_{PV}^{(val)}$). In addition, errors on stiction parameter $J$ are registered, especially with non-extended linear models (ARX, ARMAX and SS), for medium-levels disturbance. When amplitude of disturbance is high, that is, $a \in [0.5, 1]$, identification effectiveness of linear dynamics is very low with non-extended models, but stiction estimation is any-

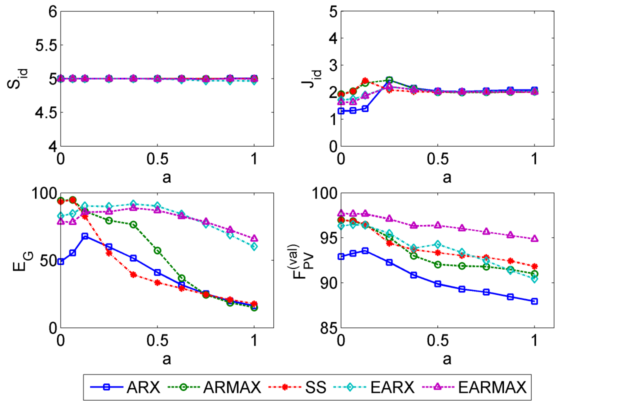


Figure 7: Simulation example: identification results for different levels of disturbance $a$. Top panel, left: $S_{id}$, right: $J_{id}$; bottom panel, left $E_G$, right $F_{PV}^{(val)}$.

way correct. Since valve input (OP) data are particularly oscillating, and therefore informative, the proposed methodologies are able to choose the correct combination of stiction parameters even though linear model is not accurate. Note also that, as expected, extended models prove to be more robust for different levels of disturbance.

### 3.2. *Effect of controller tuning*

In the case of direct identification methods, as the ones presented in this paper, the impact of controller tuning parameters on the estimation results is proved to be not particularly significant. In general, an aggressive controller tuning makes the input signal (OP) more oscillating and then more persistently exciting for the process to be identified. Whereas, a sluggish tuning produces a slowly-varying input, which is less exciting for the process, and possibly less informative for any identification procedure. The impact of controller tuning has already been studied by [27], for the identification of a pure linear dynamics without considering the problem of valve stiction. In addition, the same authors ([17], Chp. 12 in [2]), in the framework of a Hammerstein system, considered the case of double source of loop oscillation (aggressive tuning and valve stiction), by showing that the estimates of stiction parameters are still accurate.
In our study, good performances are possible for reasonably large ranges of controller parameters around nominal values, both for nonextended and extended process models. The effect of poor controller tuning has been analyzed, by using extensive simulation data and then pilot plant data. Here below only the same linear process of Section 3.1 is presented. A case of pure valve stiction, described by Kano's model with $S = 9$ and $J = 3$, is studied; no external disturbance ($\eta$) is present. Firstly, the controller parameters are set to $K_c = 1.2$ and $K_i = 1.2$, which represent an aggressive tuning. Then, the parameters are changed to $K_c = 0.2$ and $K_i = 0.2$, which compose a sluggish tuning. Note that an appropriate tuning should be $K_c = 0.5$ and $K_i = 0.5$. For both tuning settings, one hundred Monte-Carlo (MC) simulations are carried out, by using different realizations of white noise $\{e_k\}$.

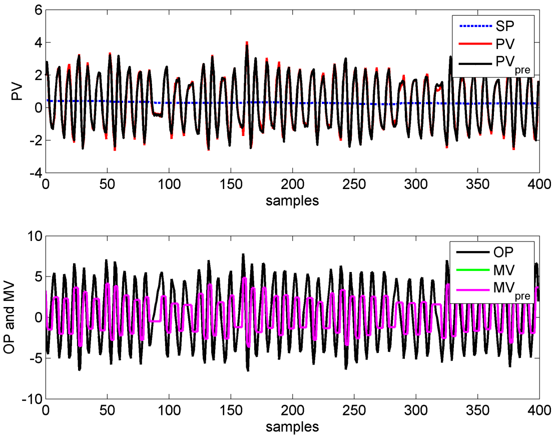


Figure 8: Simulation data with aggressive controller tuning.

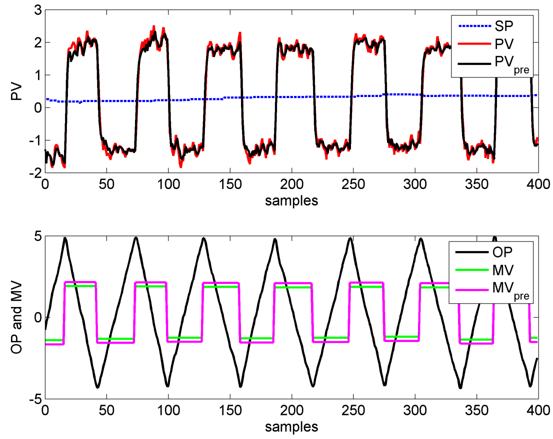


Figure 9: Simulation data with sluggish controller tuning.

Figure 8 shows the results of one identification in the case of aggressive tuning, by using Kano stiction model and ARX linear model. Figure 9 reports results of one identification in the case of sluggish tuning, by using Kano stiction model and EARX linear model. In both cases, PV and MV signals are well estimated. Similar results have been obtained for the other linear process models. Indeed, Table 1 and 2 show the overall results obtained for the two different tuning settings. Average estimates of stiction parameters ($\bar{S}$, $\bar{J}$) with corresponding standard deviations ($\sigma_S$, $\sigma_J$) are reported. Also average indices of fitting are evaluated: $\bar{F}_{PV}^{(id)}$, $\bar{F}_{PV}^{(val)}$. Therefore, good performance and robustness of the approaches with respect to very different controller tuning parameters are demonstrated.

### 3.3. Discussion of results

Main aspects and basic results of simulation study are discussed below. Firstly, it is worth noting that computational times are different for each technique. The ARX model, with a simple algorithm of LLS identification, requires much shorter times compared to ARMAX, EARX, EARMAX and SS models. There is approximately one order of magnitude: some seconds vs. some minutes.

Table 1: Results for MC simulations with aggressive tuning.

| LIN model | $\bar{S}$ | $\sigma_S$ | $\bar{J}$ | $\sigma_J$ | $\bar{F}_{PV}^{(id)}$ | $\bar{F}_{PV}^{(val)}$ |
|---|---|---|---|---|---|---|
| ARX | 9.00 | 0.00 | 2.97 | 0.05 | 99.73 | 98.71 |
| ARMAX | 9.00 | 0.00 | 2.90 | 0.06 | 98.77 | 98.75 |
| SS | 9.00 | 0.00 | 2.88 | 0.06 | 98.78 | 98.76 |
| EARX | 9.00 | 0.00 | 2.89 | 0.07 | 98.98 | 98.59 |
| EARMAX | 9.00 | 0.00 | 2.84 | 0.09 | 99.01 | 98.99 |

Table 2: Results for MC simulations with sluggish tuning.

| LIN model | $\bar{S}$ | $\sigma_S$ | $\bar{J}$ | $\sigma_J$ | $\bar{F}_{PV}^{(id)}$ | $\bar{F}_{PV}^{(val)}$ |
|---|---|---|---|---|---|---|
| ARX | 8.99 | 0.01 | 2.98 | 0.15 | 98.60 | 98.61 |
| ARMAX | 8.99 | 0.03 | 2.95 | 0.15 | 98.65 | 98.65 |
| SS | 8.99 | 0.03 | 2.93 | 0.16 | 98.67 | 98.66 |
| EARX | 8.99 | 0.01 | 2.90 | 0.27 | 98.77 | 98.40 |
| EARMAX | 9.00 | 0.00 | 2.88 | 0.23 | 98.88 | 98.90 |

Note also that in this work, for the sake of simplicity, time delay of the linear process models is never estimated. In particular, time delay is assumed known for the simulation results, and then it is fixed a priori for the pilot plant data and the industrial data (after having performed specific tests to estimate it). In the cases when time delay is unknown, it could be evaluated by considering another grid of possible time delay $L$, where $L = T_s t_d$, is taken as a multiple of the sampling time ($T_s$). For every triple $(S, J, t_d)$, the coefficients of the linear model could be then identified. This approach is robust, but obviously heavy in terms of computational load. Among other standard solutions to estimate the time delay, [22] and [27] have proposed a cross correlation analysis between the input (MV) and the output (PV) sequence. Additional simulations with unknown process time delay have showed that $t_d$ has no significant impact on the identification methods. Therefore, details are omitted in the sake of space.

In addition, it has to be recalled that the main focus of the paper is the identification and quantification of a control loop with valve stiction, possibly with the additional presence of external disturbances. So the cases of loop oscillation not due to stiction, that is, only due to aggressive controller or external disturbances or due to both of these sources, are by purpose not considered in the paper, neither in the simulation section nor for real data sets. Note also that in the industrial practice the proposed identification methods, as almost any stiction quantification method, should be applied only on data where valve stiction has been reliably detected by specific diagnosis techniques. Nevertheless, cases of pure external disturbance and pure aggressive tuning can be used as negative tests in order to estimate close-to-zero stiction parameters; this has been verified in additional simulation studies not reported in the paper for brevity.

Finally, as general results from simulation study, nonextended models prove to be better in the case of only valve stiction, while extended models outperform simpler models in the presence of additional nonstationary disturbance. These same outcomes have been obtained using different process dynamics (also with time delay estimation), other disturbance amplitudes and frequencies, other types of slowly-varying nonstationary disturbance (as drift), different trends of SP signal (also constant), and with He's stiction model in place of Kano's model. Details are omitted in the sake of space. Similar results are to be obtained on real industrial data. Note that, in general, to be able to obtain good model parameter estimates, these data have to be rich enough. Normal operating data may not be persistently exciting, especially if the set point is constant for long periods of time.

## 4. Application to a pilot plant

In this section, the efficiency of the considered methods on pilot plant data are illustrated. A diagram of the pilot plant used in the experiments is shown in Figure 10. Water circulates between drums *D1* and *D2*, and a pneumatic actuator is coupled to a spherical valve (*V2*) which controls the flow rate. Further details on the experimental apparatus can be found in [31]. The control valve, its stem and the packing are shown in Figure 10 (right). Friction is "introduced" into the valve by tightening the packing nut. The valve is equipped with a positioner, but the position control loop is open: in this way the actual valve stem position (MV) is measured but the positioner does not perform any control action. The PV is the flow rate through the valve and the OP is the output signal from a PI controller. The opening of the valve *V3* (installed downstream the sticky valve *V2*) is changed by imposing, as command (OP), a near sinusoidal profile in order to "generate" the external disturbance.

Three different sets of data are collected with a sampling time of 1 s.

*I.* A low amount of valve stiction is the only source of oscillation.

*II.* A high amount of stiction is introduced around the valve stem.

*III.* An external disturbance is introduced and acts simultaneously with stiction of low amount.

Figure 11 (left) shows the MV(OP) diagram of the valve obtained imposing triangular waves on OP, oscillating from 0 to 100% of the valve span, when a low amount of stiction is applied to the stem. On the right of Figure 11 the same diagram is shown, when a high amount of stiction is applied.

The valve shows an asymmetric behavior: $S$ (dead-band + stick-band) is bigger in the closing direction and smaller in the opening direction, while the slip jump $J$ is always really small. The stiction parameters obtained from these off-line (manual) tests on the valve are approximately known: $S \in [13, 15]$, $J \in [0.1, 0.2]$ in the case of low stiction, and $S \in [22, 29]$, $J \in [0.2, 1]$ in the case of high stiction.

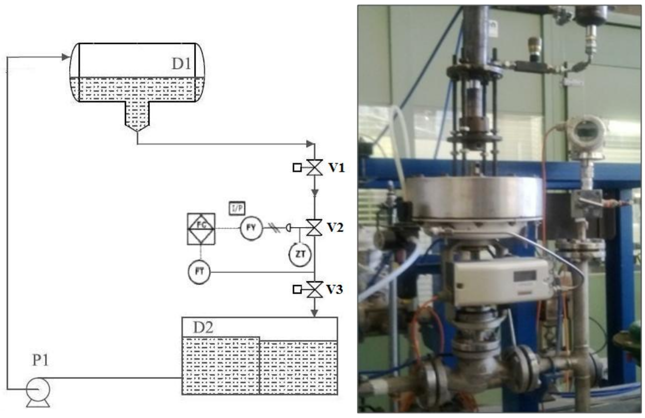


Figure 10: Pilot plant: process diagram (left) and a picture of the sticky valve (right).

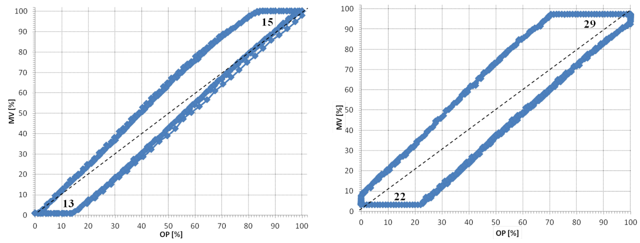


Figure 11: Pilot plant: experimental behavior MV vs. OP in the case of low stiction (left) and high stiction (right).

Kano's model and He's model are used to fit the *measured* MV signals of the three sets of data collected in closed loop. The best combinations of parameters are, in the case of low stiction, $S = (f_s + f_d) = 12.1$, $J = (f_s - f_d) = 0.1$ (both for Kano's and He's model), with a fitting index $F_{MV} = 71.75\%$. In the case of high stiction, actual stiction parameters are $S = 22.1$, $J = 0.2$ (for Kano's), with a fitting of 76.28%, and $S = 22.0$, $J = 0.1$ (for He's), with a fitting of 76.27%. Therefore, both nonlinear models appear sufficiently adequate.

The five linear process models with the two stiction models are then applied to detect and quantify the amount of stiction without the knowledge of the MV signal. The time delay and the orders of the linear process models are fixed *a priori*, namely $t_d = 5$, $(n,m) = (2,2)$ for ARX and EARX, $(n,m,p) = (2,2,2)$ for ARMAX and EARMAX, $n = 2$ for SS. Table 3, 4 and 5 show respectively the results of the comparison for the first, the second and the third experimental set.

*Test 1.* In Table 3, identification results obtained with all ten combinations of models are reported. In all cases good estimates of the nonlinearity are established: $F_{MV} \in [60\%, 70\%]$, and $(S,J)$ are close to their actual values. EARMAX and EARX models perform also a better PV fitting. Figure 12 shows the registered time trends of SP, PV, OP, MV and the estimated values of PV and MV ($PV_{est}$, $MV_{est}$) of the first experiment when Kano's model for the sticky valve and EARX model for the linear dynamics are used. Both the PV fitting indices are sufficiently high (cf. Table 3): $F_{PV}^{(id)} = 88.31\%$ for the identifi-

Table 3: Pilot plant first experiment: low amount of valve stiction.

| LIN model | NL model | $S$ | $J$ | $F_{PV}^{(id)}$ | $F_{PV}^{(val)}$ | $F_{MV}$ |
|---|---|---|---|---|---|---|
| ARX | Kano | 11.9 | 0.2 | 86.03 | 84.70 | 69.35 |
| | He | 11.8 | 0.1 | 86.01 | 84.63 | 69.25 |
| ARMAX | Kano | 11.9 | 0.2 | 86.08 | 84.72 | 67.54 |
| | He | 11.8 | 0.2 | 86.07 | 84.56 | 69.05 |
| SS | Kano | 12.5 | 0.1 | 85.88 | 84.77 | 69.09 |
| | He | 12.9 | 1.0 | 85.88 | 84.29 | 60.46 |
| EARX | Kano | 11.9 | 0.2 | 88.31 | 82.95 | 69.35 |
| | He | 11.4 | 0.4 | 88.49 | 82.65 | 60.77 |
| EARMAX | Kano | 11.9 | 0.2 | 88.52 | 84.03 | 69.35 |
| | He | 11.4 | 0.4 | 88.57 | 83.74 | 60.77 |

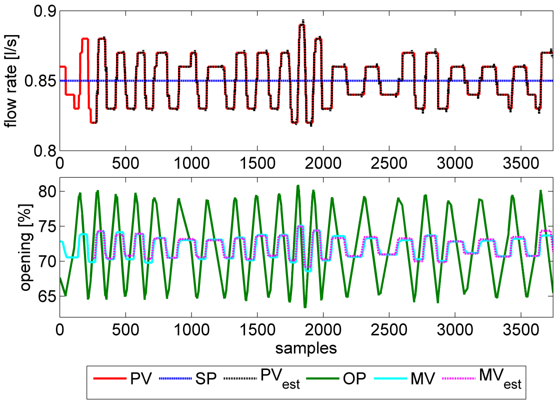


Figure 12: Pilot plant first experiment: registered time trends.

cation dataset and $F_{PV}^{(val)} = 82.95\%$ for the validation dataset. Also the estimation of the valve stem position is quite accurate: $F_{MV} = 69.35\%$. In this first experiment, with only valve stiction, both nonextended (ARX, ARMAX, SS) and extended models (EARX, EARMAX) are appropriate to the purpose.

*Test 2.* Table 4 shows that good estimation results are obtained again with nonextended (ARX, ARMAX and SS) models. They guarantee a better identification of the nonlinearity: $F_{MV}$ values are higher. EARMAX and EARX models perform a slightly higher PV fitting but, in this case, produce a significantly worse MV estimation: $F_{MV} \in [25\%, 42\%]$. Since these two models have one more degree of freedom, they tend to generate a bias term ($\eta$) even though the external disturbance is not present in order to improve the PV fitting, but this alters the stiction quantification. Figure 13 shows the corresponding registered time trends and estimated signals of the second experiment when He's model and the SS model are used. Both the PV fitting indices are high (cf. Table 4): $F_{PV}^{(id)} = 85.77\%$ for the identification dataset and $F_{PV}^{(val)} = 83.68\%$ for the validation dataset. The estimation of the valve stem position is rather accurate: $F_{MV} = 71.82\%$. Non extended models prove themselves most appropriate when only valve stiction is present in the control loop.

Table 4: Pilot plant second experiment: high amount of valve stiction.

| LIN model | NL model | $S$ | $J$ | $F_{PV}^{(id)}$ | $F_{PV}^{(val)}$ | $F_{MV}$ |
|---|---|---|---|---|---|---|
| ARX | Kano | 25.2 | 4.3 | 85.53 | 83.57 | 62.61 |
| | He | 23.6 | 1.5 | 85.59 | 83.99 | 63.44 |
| ARMAX | Kano | 24.5 | 3.5 | 85.62 | 84.27 | 71.85 |
| | He | 22.7 | 2.0 | 85.77 | 83.79 | 71.82 |
| SS | Kano | 24.5 | 3.5 | 85.67 | 84.26 | 71.85 |
| | He | 22.7 | 2.0 | 85.77 | 83.68 | 71.82 |
| EARX | Kano | 26.6 | 0.7 | 87.07 | 83.65 | 28.93 |
| | He | 25.0 | 1.6 | 87.25 | 83.63 | 41.39 |
| EARMAX | Kano | 26.8 | 3.3 | 87.37 | 82.22 | 25.33 |
| | He | 25.0 | 1.6 | 87.34 | 83.70 | 41.39 |

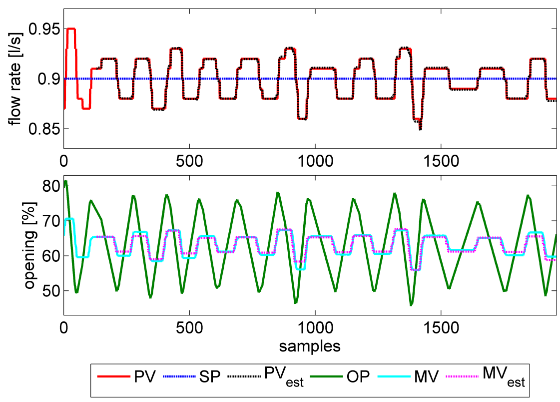


Figure 13: Pilot plant second experiment: registered time trends.

*Test 3.* The results of the third experiment are basically opposite to those of the second experiment (cf. Table 5). EARMAX and EARX models ensure both a better PV fitting and a higher MV estimation. On the contrary, nonextended models perform a lower identification of the global dynamics and a wrong estimation of the nonlinearity. For the validation dataset, SS model produces instable trends in $PV_{est}$ and $F_{PV}^{(val)}$ indices tend to minus infinite. The presence of a large external disturbance can alter significantly stiction estimation when a nonextended model is used to identify the linear dynamics.

Figure 14 shows the signals of the third experiment when He's model and the EARMAX model are used. In the bottom panel the stem position of valve *V3* is reported; this signal is proportional to the disturbance entering the process. The extended model gives an accurate PV fitting (cf. Table 5), $F_{PV}^{(id)} = 86.50\%$, $F_{PV}^{(val)} = 83.54\%$, and a good MV fitting $F_{MV} = 72.10\%$, much higher compared to values obtained with ARX, ARMAX and SS models. The estimated stiction values obtained with EARX and EARMAX are close to the real parameters ($S \simeq 13.1; J \simeq 0.5$) unlike those obtained with nonextended models. Therefore, the additional presence of an external disturbance can be well managed when an extended model is used for stiction estimation.

As general conclusion, the results obtained with pilot plant

Table 5: Pilot plant third experiment: low amount of valve stiction and external disturbance.

| LIN model | NL model | $S$ | $J$ | $F_{PV}^{(id)}$ | $F_{PV}^{(val)}$ | $F_{MV}$ |
|---|---|---|---|---|---|---|
| ARX | Kano | 23.7 | 3.1 | 84.91 | 85.19 | 49.28 |
| | He | 22.0 | 4.4 | 85.38 | 83.94 | 46.86 |
| ARMAX | Kano | 23.7 | 0.7 | 85.21 | 84.65 | 47.37 |
| | He | 22.0 | 4.4 | 85.46 | 84.04 | 46.86 |
| SS | Kano | 17.1 | 2.9 | 85.50 | $-\infty$ | 69.66 |
| | He | 17.0 | 2.2 | 85.50 | $-\infty$ | 67.82 |
| EARX | Kano | 14.7 | 0.2 | 86.12 | 83.62 | 74.25 |
| | He | 15.2 | 2.1 | 86.38 | 83.80 | 73.25 |
| EARMAX | Kano | 14.8 | 2.0 | 86.24 | 82.93 | 73.81 |
| | He | 12.4 | 4.3 | 86.50 | 83.54 | 72.10 |

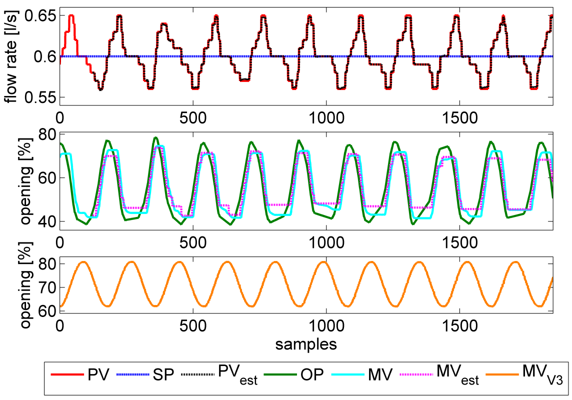


Figure 14: Pilot plant third experiment: registered time trends.

data have basically confirmed the ones achieved with simulation data.

## 5. Application to industrial data

In this section, the performance of the proposed methods are further compared on some different industrial datasets.

### *5.1. Data from benchmark [2]*

Three loops of the dataset of the book of [2], illustrated as a benchmark for stiction detection methods, are firstly used. These three loops are clearly indicated as suffering from valve stiction by several detection methods [2]. The five proposed linear process models are tested, while only Kano's model is used to describe the sticky valve dynamics. Unless otherwise specified, datasets are used in full: the first two-thirds of data are used as identification set and the last-third is used as validation set. The time delay and the linear models orders are fixed: $t_d = 1$, $(n,m) = (2,2)$ for ARX and EARX, $(n,m,p) = (2,2,2)$ for ARMAX and EARMAX, $n = 2$ for SS. These data are also used purposely to show the effect of the initialization of Kano's model on stiction estimates.

The results are then compared with the estimates given by some well-established literature procedures: (i) Karra and Karim [17], (ii) Jelali [21], (iii) Lee at. al [22], (iv) Romano and Garcia [24]. Note that the proposed EARMAX-Kano model is directly comparable with [17], since both use a recursive least-squares (RLS) algorithm. In addition, the proposed ARMAX-Kano model is quite close to the approach of [21], which but uses global optimization algorithms to get the solution. Finally, the method of [24] employs a different model structure (Hammerstein-Wiener), which tends to produce results farther from others.

*CHEM 25.* The data of this pressure control loop were obtained from a refinery. Karra and Karim used the following parameters for their EARMAX model: $t_d = 1$ and $(n,m,p) = (2,2,2)$. Jelali tested the loop twice using an ARMAX model with: (i) $t_d = 2$, $(n,m,p) = (3,2,2)$ and (ii) $t_d = 1$, $(n,m,p) = (2,2,1)$. Romano and Garcia tested 272 non specified samples without reporting the exact model parameters. Lee et al. used a second order linear model, that is, an ARX with $(n,m) = (2,1)$, and He's stiction model on a specific data window (100 - 350 samples).

Table 6 summarizes the estimates obtained using the proposed models and the results available in the literature. The estimates of $(S,J)$ with all methods are really close. Only Lee et al. obtain a higher value of $J$, probably due to the use of He's model. The proposed EARMAX model (case *a*) gives exactly the same stiction estimate of Karra and Karim once that Kano's model is initialized as in the literature work. Using In.2 initialization discussed in 2.4, slightly different values of $S$ and $J$ are obtained (case *b*). It should be also noted that the proposed EARX and EARMAX models produce the highest values of PV fitting.

*CHEM 10.* These data come from a pressure control loop in a chemical process industry. Karra and Karim used the following parameters for their EARMAX model: $t_d = 1$ and $(n,m,p) = (2,2,2)$ [2, Chp. 12]. Lee et al. used an ARX$(2,1)$ and He's stiction model.

Table 7 summarizes all the results. The estimates of $S$ are very close in all the five proposed methods, while the estimates of $J$ are bit more variable. These results are obtained with In.2 initialization of Section 2.4 setting the *stationary time* of MV at the first tenth of the data length. Also Lee et al. obtained similar values of $S$ and $J$, while Karra and Karim obtained a similar value of $S$ but a smaller value of slip-jump ($J = 0.05$). In particular, for this dataset, as showed for EARMAX model, different stiction estimates are possible using four different Kano's model initializations of type In.1 (cf. Figure 4). Note that values close-to-zero of stiction are incorrectly obtained with a specific initialization: $stp = 0; d = -1$.

*POW 4.* These data are from a level control loop in a power plant. Karra and Karim used an EARMAX model with unspecified parameters applied on an initial data window (1 - 1000 samples). Jelali tested the loop using an ARMAX model of unspecified orders, probably on the first 700 samples. Lee et al. used an ARX$(2,1)$ and He's stiction model applied on all available data. The proposed identification methods are executed on

Table 6: CHEM 25: comparison of results.

| LIN model | NL model | $S$ | $J$ | $F_{PV}^{(id)}$ | $F_{PV}^{(val)}$ |
|---|---|---|---|---|---|
| ARX | Kano | 1.8 | 0.3 | 74.14 | 72.96 |
| ARMAX | Kano | 1.8 | 0.2 | 74.45 | 73.79 |
| SS | Kano | 2.0 | 0.2 | 73.88 | 73.55 |
| EARX | Kano | 1.8 | 0.3 | 78.67 | 73.92 |
| EARMAX (*a*) | Kano | 1.8 | 0.3 | 78.83 | 73.95 |
| EARMAX (*b*) | Kano | 1.6 | 0.0 | 79.32 | 74.09 |
| Karra & Karim [17] | Kano | 1.8 | 0.3 | - | - |
| Jelali (i) [21] | Kano | 1.80 | 0.59 | - | - |
| Jelali (ii) [21] | Kano | 1.87 | 0.60 | - | - |
| Romano & Garcia [24] | Kano | 1.60 | 0.44 | 68.70 | - |
| Lee et al. [2, Chp. 13] | He | 1.62 | 1.62 | - | - |

Table 7: CHEM 10: comparison of results.

| LIN model | NL model | $S$ | $J$ | $F_{PV}^{(id)}$ | $F_{PV}^{(val)}$ |
|---|---|---|---|---|---|
| ARX | Kano | 1.85 | 1.70 | 93.21 | 92.86 |
| ARMAX | Kano | 1.85 | 1.50 | 93.50 | 92.92 |
| SS | Kano | 1.85 | 1.70 | 93.63 | 92.87 |
| EARX | Kano | 1.90 | 1.45 | 93.79 | 91.33 |
| EARMAX | Kano | 1.85 | 1.35 | 93.85 | 92.55 |
| EARMAX ($stp = 1; d = 1$) | Kano | 1.85 | 1.80 | 93.83 | 92.55 |
| EARMAX ($stp = 1; d = -1$) | Kano | 1.90 | 1.75 | 94.10 | 91.16 |
| EARMAX ($stp = 0; d = 1$) | Kano | 1.85 | 1.65 | 93.60 | 92.28 |
| EARMAX ($stp = 0; d = -1$) | Kano | 0.20 | 0.10 | 93.34 | 91.63 |
| Karra & Karim [2, Chp. 12] | Kano | 1.85 | 0.05 | - | - |
| Lee et al. [2, Chp. 13] | He | 1.77 | 1.73 | - | - |

the first 1000 samples, with In.2 initialization of Section 2.4 and setting the *stationary time* of MV at the first tenth of the data length.

Table 8 summarizes all the results. For this loop, the estimates of stiction parameters are different with the five proposed methods. ARX, ARMAX and SS models agree and estimate low values of stiction: $S \in [0.8, 0.9]$, $J = 0$. Conversely, EARX and EARMAX models yield larger amounts: $S = 4.1$, $J \in [0.4, 0.7]$. Also Lee et al. obtained low values, while Karra and Karim estimated a much more significant amount of stiction and they also assessed the presence of an external disturbance. For this case, it can be observed that techniques which implement an extended process model yield higher stiction values than techniques which use a nonextended model. The first ones also identify a significant additional disturbance, which alters numerical estimates of stiction. Note that Jelali obtained the largest stiction amount, since his final value of $S$ falls close to the initial guess ($S_0 = 4.80$) obtained with the ellipse-fitting method [32].

As overall considerations, since there is no information about the real values of $S$ and $J$, it is not possible to say exactly which are the best estimates. However, for the first two applications, as the stiction estimates in all proposed methods are close and next to the values reported in some well-established literature works, it is possible to conclude that all the techniques give acceptable results. In particular, the estimates of $S$ are very close and therefore really reliable. The estimates of $J$ are more variable and therefore, as expected and previously discussed, more difficult. Moreover, the initialization of Kano's model is proved to be a factor which can alter stiction estimates. The third application clearly confirms that different techniques can also strongly disagree when applied on the same industrial data [2, Chp. 13]. Some other examples of comparison of selected stiction quantification techniques applied on benchmark data are reported in [33].

Table 8: POW 4: comparison of results.

| LIN model | NL model | $S$ | $J$ | $F_{PV}^{(id)}$ | $F_{PV}^{(val)}$ |
|---|---|---|---|---|---|
| ARX | Kano | 0.9 | 0.0 | 84.82 | 84.29 |
| ARMAX | Kano | 0.9 | 0.0 | 84.80 | 84.33 |
| SS | Kano | 0.8 | 0.0 | 85.19 | 84.78 |
| EARX | Kano | 4.1 | 0.7 | 85.95 | 82.37 |
| EARMAX | Kano | 4.1 | 0.4 | 86.13 | 82.70 |
| Karra & Karim [2, Chp. 13] | Kano | 3.6 | 1.2 | - | - |
| Jelali [21] | Kano | 4.49 | 2.49 | - | - |
| Lee et al. [2, Chp. 13] | He | 0.58 | 0.39 | - | - |

### 5.2. *Data from other industrial loops*

The proposed identification techniques are then applied to three datasets obtained during multiannual application of a performance monitoring software [34] in Italian refinery and petrochemical industries. Data refer to repeated registrations (of PV, OP, SP) for the same loops. The source of malfunction is known to be stiction, but the actual MV signals are not available. Trends of values of parameter $S$ are reported for each combination of nonlinear and linear model. Values of $J$ are not reported since their estimate, as shown previously, is less significant and reliable.

*Loop I.* These data were previously presented in [18], as application of the original grid search technique and the first identification method (ARX model). For this pressure control loop, six different registrations, collected during a month, are available just before the valve maintenance. Four detection techniques ([10, 13, 15, 16]) indicate this loop as always affected by stiction in these acquisitions. Therefore, rather constant stiction values, though unknown, are expected. In Figure 15 pretty uniform values of stiction ($S \in [4, 5.6]$) are obtained for each combination of nonlinear and linear models. Low variability in estimated values of $S$ is given by all linear models plus Kano's model. SS model plus Kano's model gives the lowest variability ($\sigma_S = 0.23$) with a mean value ($\hat{S} = 5.36$) higher than other techniques. Slightly higher variability is obtained with He's model, especially with SS model. Figure 16 shows time trends of SP, PV, OP and estimated values of PV and MV ($PV_{est}$, $MV_{est}$) of registration # 3 when Kano's model and EARMAX model are used.

The results of this industrial application reproduces the outcome of the first experimental set in the pilot plant (cf. Table 3),

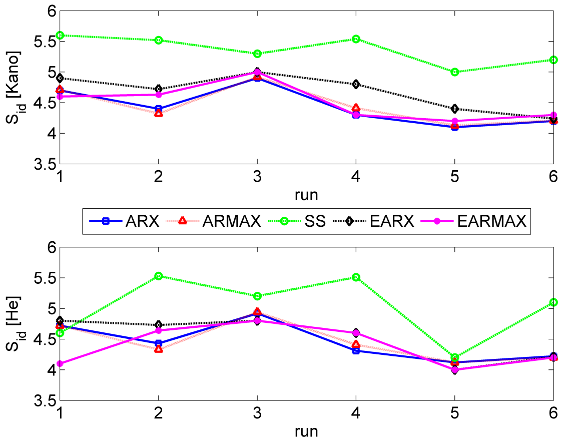


Figure 15: Industrial Loop I: Trends of the identified stiction parameter $S$ using different linear models: top, Kano's model; bottom, He's model.

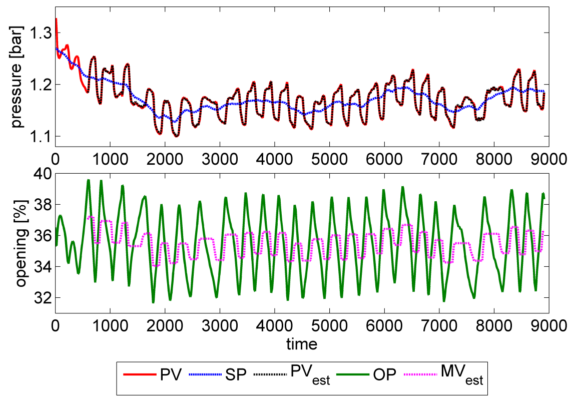


Figure 16: Industrial Loop I: time trends for registration # 3.

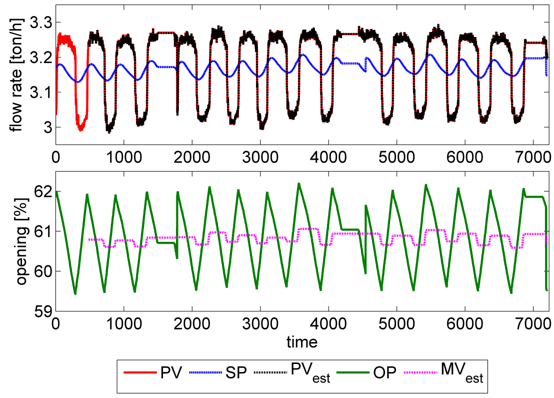


Figure 17: Industrial Loop II: time trends for registration # 9.

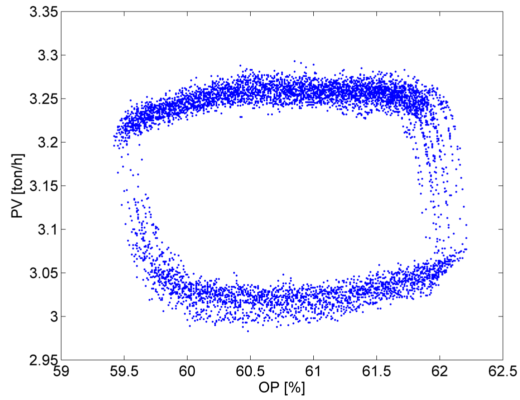


Figure 18: Industrial Loop II: experimental behavior PV vs. OP obtained in registration # 9.

where all the linear models are equally valid. In this application, all the identification techniques prove to be sufficiently reliable: constant stiction trends are always estimated. Note that slightly decreasing trends of stiction are anyway admissible. Here the SP is variable (Figure 16), therefore stiction could be not exactly the same for different operating conditions along the same registration or - more likely - along different acquisitions, while Kano's and He's models imply uniform parameters for the whole valve span.

*Loop II.* These data are from a flow rate control loop with PI-algorithm controller and variable set point. The presence of stiction is clearly recognizable by the PV and OP shapes being close to squared and triangular waves, respectively (Figure 17). Moreover, the plot of PV(OP) shows evident stiction characteristics (Figure 18), since in FC loops PV is proportional to MV. The same four detection techniques ([10, 13, 15, 16]) indicate this loop as affected by stiction in 11 acquisitions registered along two consecutive days. Therefore, nearly constant stiction values, though unknown, are expected. From Figure 19, rather uniform values of stiction ($S \in [1.8, 2.5]$) are quantified with nonextended models. The lowest variability in estimated values of $S$ is given by ARMAX and SS models plus Kano's or He's model ($\sigma_S \in [0.13, 0.14]$) with a mean value $\hat{S} \in [2.26, 2.30]$. Conversely, an excessively high variability is obtained using extended models: EARX and EARMAX.

The results of this industrial application are rather similar to the outcome of the second experimental set in the pilot plant (cf. Table 4), where the nonextended models are more appropriate for the case of only valve stiction. Extended models prove to be not sufficiently reliable: high variable stiction trends are estimated. Sometimes even zero values are obtained: loop oscillation is not associated with valve stiction but wrongly with a significant bias term of external disturbance.

*Loop III.* These data are from a flow rate control loop, the controller has a PID algorithm, and the SP is variable since the loop is the inner part of a cascade control. The same four detection techniques ([10, 13, 15, 16]) indicate stiction in 6 acquisitions registered along four months. Therefore, a constant or increasing trend of stiction is expected. Once again the presence of stiction is clearly recognizable by the shapes of PV and OP signals, being close to squared and triangular waves, respectively (Figure 20). Now, for this loop, the two extended models (EARX and EARMAX) give rather uniform values of stiction ($S \in [2.1, 3.1]$). Conversely, for registration # 4, using ARX and ARMAX models, and for # 5, using all three nonextended models, very low ($S \simeq 0$) or low values are estimated (see Fig-

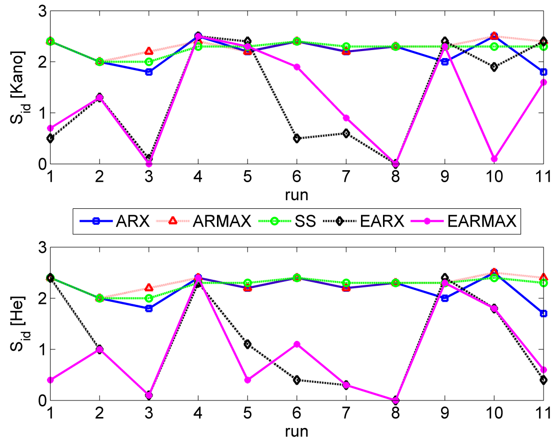


Figure 19: Industrial Loop II: Trends of the identified stiction parameter $S$ using different linear models: top, Kano's model; bottom, He's model.

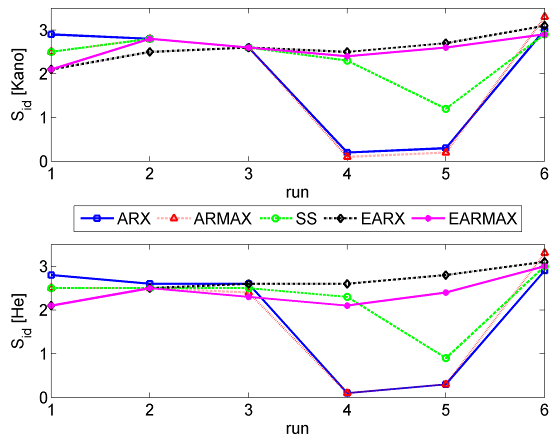


Figure 21: Industrial loop III: Trends of the identified stiction parameter $S$ using different linear models: top, Kano's model; bottom, He's model.

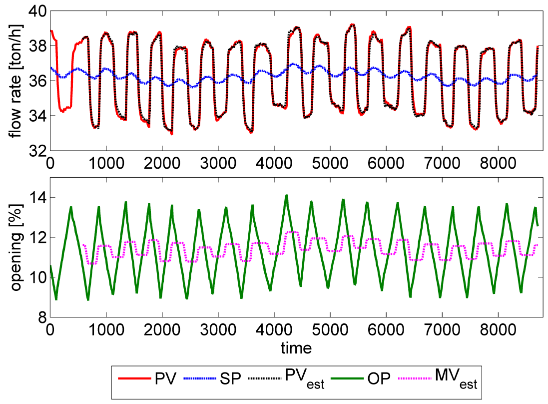


Figure 20: Industrial Loop III: time trends for registration # 2.

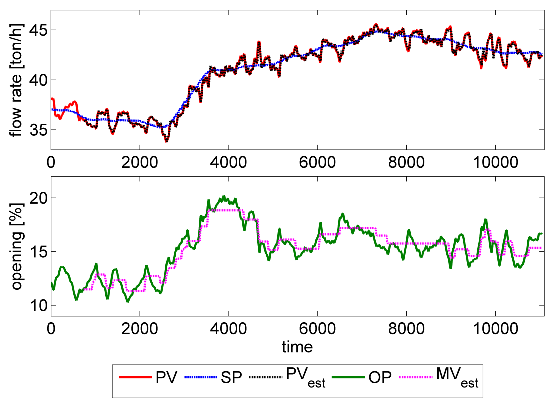


Figure 22: Industrial Loop III: time trends for registration # 4.

ure 21). These estimates appear incorrect since they result as outliers with respect to the main stiction trend. In these two registrations, PV signal does not clearly show a singular frequency of oscillation (cf. Figure 22). An external disturbance might act simultaneously with valve stiction.

The results of this last industrial application are rather similar to the outcome of the third experimental set in the pilot plant (cf. Table 5), where extended models are to be preferred for the case of simultaneous valve stiction and external disturbance. Non extended models are not sufficiently reliable: inconsistent values of stiction can be estimated. The loop oscillation is not due to a singular frequency and external disturbance can alter stiction estimation.

As a general conclusion, the results obtained with industrial data confirm those achieved with pilot plant data. Nonextended models are the best choice when valve stiction is the only source of loop oscillation; extended models are better for the case of simultaneous presence of external disturbances. It is worth noting that for industrial data the presence (or the absence) of non stationary disturbances is not known a priori. Nevertheless, repeated data acquisitions for the same valve can help since they allow one to perform comparable estimates, that is, time evolution of stiction can be followed and eventual anomalous cases can be assessed. For example, outliers can be ascribed to the presence of disturbances whether non extended models are used, or, on the opposite, the absence of disturbances can be inferred whether inconsistent estimates are obtained when extended models are tested. Anyway, this criterion could be not reasonable when only few acquisitions, or even just one, are available. In such cases a conservative approach should be to test all different models and then emit an average verdict. Thus, a reliable detection of additional external disturbances seems the definitive solution to this problem. Recent techniques [35, 36] allow one to detect multiple oscillation. Therefore, they could be used as a preliminary step in stiction estimation in order to assess the simultaneous presence of different sources of oscillation (stiction and disturbance) and to direct the choice between simpler and extended process models.

## 6. Conclusions

In this paper the effect of nonstationary disturbances on estimated amount of stiction has been investigated. For this reason, two different stiction models and five linear models are proposed and compared in order to identify the Hammerstein system of the sticky valve and the process. The identification methods have been validated, firstly, by using closed-loop simulation data in the presence of different faults (low/high stiction, with/without external non-stationary disturbances). Then, practical applicability and significance has been demonstrated through the application of the considered identification methods to data obtained from a pilot plant and to a large number of industrial loops.

For the nonlinear part, both Kano's and He's models confirm to be appropriate to model the sticky valve. Simpler models (ARX, ARMAX and SS) appear to be the best choice for linear process dynamics when stiction is the only source of loop oscillation. Extended models (EARX and EARMAX), incorporating the time varying additive nonstationary disturbance, have one more degree of freedom, i.e. the bias term which is estimated recursively along with the process and stationary noise parameters. When the external disturbance is actually present, extended models prove to be very effective and generate consistent stiction model parameters. As a matter of fact, as verified by different types of industrial data, the extended models ensure a better process identification and a more accurate stiction estimation in the case of significant disturbances acting simultaneously with valve stiction.

Future research directions may include the application of recent techniques aimed at detecting the presence of large external disturbances in order to choose between extended and nonextended models. Furthermore, more complex and flexible stiction models could be used to describe non uniform friction dynamics in order to obtain more consistent estimates when repeated data registrations are analyzed.

## References


[1] R. Bacci di Capaci, C. Scali, G. Pannocchia, Identification techniques for stiction quantification in the presence of nonstationary disturbances, in: Proceedings of 9th IFAC ADCHEM, Whistler, Canada, 2015, pp. 629–634.

[2] M. Jelali, B. Huang, Detection and Diagnosis of Stiction in Control Loops: State of the Art and Advanced Methods, Springer-Verlag, London, 2010.

[3] M. A. A. S. Choudhury, S. L. Shah, N. F. Thornhill, Modelling valve stiction, Contr. Eng. Pract. 13 (2005) 641–658.

[4] D. Karnopp, Computer simulations of stick-slip friction in mechanical dynamics systems, Trans. ASME J. Dyn. Syst., Meas., Control 107 (1985) 100–103.

[5] C. Canudas de Wit, H. Olsson, K. Åström, P. Lischinsky, A new model for control of systems with friction, IEEE Trans. Autom. Control 40 (1995) 419–425.

[6] A. Stenman, F. Gustafsson, K. Forsman, A segmentation-based method for detection of stiction in control valves, Int. J. Adapt. Control 17 (2003) 625–634.

[7] M. Kano, M. Hiroshi, H. Kugemoto, K. Shimizu, Practical model and detection algorithm for valve stiction, in: Proceedings of 7th IFAC DYCOPS, Boston, USA, 2004, paper ID n. 54.

[8] Q. P. He, J. Wang, M. Pottmann, S. J. Qin, A curve fitting method for detecting valve stiction in oscillating control loops, Ind. Eng. Chem. Res. 46 (2007) 4549–4560.

[9] S. L. Chen, K. K. Tan, S. Huang, Two-layer binary tree data-driven model for valve stiction, Ind. Eng. Chem. Res. 47 (2008) 2842–2848.

[10] A. Horch, A simple method for detection of stiction in control valves, Contr. Eng. Pract. 7 (1999) 1221–1231.

[11] R. Srinivasan, R. Rengaswamy, R. Miller, Control loop performance assessment. 1. a qualitative approach for stiction diagnosis, Ind. Eng. Chem. Res. 44 (2005) 6708–6718.

[12] A. Singhal, T. I. Salsbury, A simple method for detecting valve stiction in oscillating control loops, J. Proc. Contr. 15 (2005) 371–382.

[13] M. Rossi, C. Scali, A comparison of techniques for automatic detection of stiction: Simulation and application to industrial data, J. Proc. Contr. 15 (2005) 505–514.

[14] Y. Yamashita, An automatic method for detection of valve stiction in process control loops, Contr. Eng. Pract. 14 (2006) 503–510.

[15] C. Scali, C. Ghelardoni, An improved qualitative shape analysis technique for automatic detection of valve stiction in flow control loops, Contr. Eng. Pract. 16 (2008) 1501–1508.

[16] M. A. A. S. Choudhury, S. L. Shah, N. F. Thornhill, Diagnosis of poor control loop performance using higher order statistics, Automatica 40 (2004) 1719–1728.

[17] S. Karra, M. N. Karim, Comprehensive methodology for detection and diagnosis of oscillatory control loops, Contr. Eng. Pract. 17 (2009) 939–956.

[18] R. Bacci di Capaci, C. Scali, Stiction quantification: A robust methodology for valve monitoring and maintenance scheduling, Ind. Eng. Chem. Res. 53 (2014) 7507–7516.

[19] R. Srinivasan, R. Rengaswamy, S. Narasimhan, R. Miller, Control loop performance assessment. 2. hammerstein model approach for stiction diagnosis, Ind. Eng. Chem. Res. 44 (2005) 6719–6728.

[20] M. A. A. S. Choudhury, S. L. Shah, N. F. Thornhill, D. S. Shook, Stiction - definition, modelling, detection and quantification, J. Proc. Contr. 18 (2008) 232–243.

[21] M. Jelali, Estimation of valve stiction in control loops using separable last square and global search algorithms, J. Proc. Contr. 18 (2008) 632–642.

[22] K. H. Lee, Z. Ren, B. Huang, Novel closed-loop stiction detection and quantification method via system identification, in: Proceedings of the 3rd ADCONIP, Jasper, Alberta, Canada, 2008, pp. 341–346.

[23] M. Farenzena, J. O. Trierweiler, Valve stiction evaluation using global optimization, Contr. Eng. Pract. 20 (2012) 379–385.

[24] R. A. Romano, C. Garcia, Valve friction and nonlinear process model closed-loop identification, J. Proc. Contr. 21 (2011) 667–677.

[25] A. P. Araujo, C. J. Munaro, M. R. Filho, Quantification of valve stiction and dead band in control loops based on the harmonic balance method, Ind. Eng. Chem. Res. 51 (2012) 14121–14134.

[26] Q. P. He, J. Wang, Valve stiction quantification method based on a semi-physical valve stiction model, Ind. Eng. Chem. Res. 53 (2014) 12010–12022.

[27] S. Karra, M. N. Karim, Alternative model structure with simplistic noise model to identify linear time invariant systems subjected to non-stationary disturbances, J. Proc. Contr. 19 (2009) 964–977.

[28] J. Wang, Q. Zhang, Detection of asymmetric control valve stiction from oscillatory data using an extended hammerstein system identification method, J. Proc. Contr. 24 (2014) 1–12.

[29] L. Fang, J. Wang, Identification of hammerstein systems using preisach model for sticky control valves, Ind. Eng. Chem. Res. 54 (2015) 1028–1040.

[30] G. Pannocchia, M. Calosi, A predictor form PARSIMonious algorithm for closed-loop subspace identification, J. Proc. Contr. 20 (2010) 517–524.

[31] R. Bacci di Capaci, C. Scali, D. Pestonesi, E. Bartaloni, Advanced diagnosis of control loops: Experimentation on pilot plant and validation on industrial scale, in: Proceedings of 10th IFAC DYCOPS, Mumbai, India, 2013, pp. 589–594.

[32] M. A. A. S. Choudhury, S. L. Shah, N. F. Thornhill, D. S. Shook, Automatic detection and quantification of stiction in control valves, Control Engineering Practice 16 (2006) 1395–1412.

[33] R. B. di Capaci, Advanced diagnostic of industrial process control systems, Ph.D. thesis, Chemical Engineering, University of Pisa (2016).

[34] C. Scali, M. Farnesi, Implementation, parameters calibration and field validation of a closed loop performance monitoring system, Annu. Rev. Contr. 34 (2010) 263–276.

[35] E. Naghoosi, B. Huang, Automatic detection and frequency estimation of oscillatory variables in the presence of multiple oscillations, Ind. Eng. Chem. Res. 53 (2014) 9247–9438.

[36] Z. Guo, L. Xie, A. Horch, Y. Wang, H. Su, X. Wang, Automatic detection of nonstationary multiple oscillations by an improved wavelet packet transform, Ind. Eng. Chem. Res. 53 (2014) 15686–15697.